THE JOURNAL OF PHYSICAL CHEMISTRY A

Article

pubs.acs.org/JPCA

Reactions of Neutral Platinum Clusters with N_2O and CO

Hirotaka Yamamoto, Ken Miyajima, Tomokazu Yasuike,† and Fumitaka Mafuné*

Department of Basic Science, Graduate School of Arts and Sciences, The University of Tokyo, Komaba, Meguro-ku, Tokyo 153-8902, Japan

Supporting Information

ABSTRACT: The reduction of N_2O in the gas phase by isolated, neutral platinum clusters, Pt_n (n = 4−12), was investigated using mass spectrometry. The associated oxygen transfer reactions had the general formula $Pt_nO_{m-1} + N_2O \rightarrow Pt_nO_m + N_2$ (m = 1 or 2). The rate constants k_1 and k_2 for the reactions in which m = 1 and 2, respectively, were ascertained and were found to be similar to one another. Unexpectedly, Pt_6O was discovered to be completely unreactive with N_2O under the applied experimental conditions. The reaction mechanism was elucidated on the basis of density functional theory (DFT) calculations, which indicated a reaction barrier between $Pt_6O + N_2O$ and $Pt_6O_2 + N_2$. The possibility of catalyzing either the reduction of N_2O or the oxidation of CO using neutral Pt_n species was also examined and the results showed that Pt_n does not exhibit significant catalytic properties and that O and CO instead coadsorb to Pt_n. Desorption of CO_2 from the coadsorbed clusters was not clearly identifiable from mass spectra. The reactivities of the platinum clusters were discussed and compared with the properties of the highly catalytically active rhodium clusters.

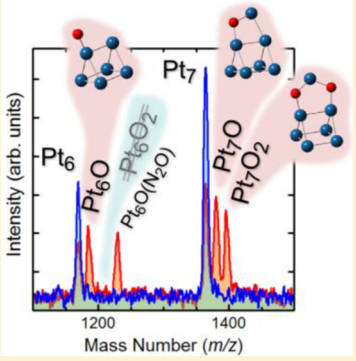

INTRODUCTION

Platinum is widely used as a catalyst in numerous chemical reactions. It plays an important role as a heterogeneous catalyst in hydrogenation and dehydrogenation reactions,[1] for example, and platinum is a vital component of automotive three-way catalytic converters.[2−6] Despite the importance of platinum in catalysis, there have been only a very limited number of spectroscopic studies of its clusters in the gas phase.[7,8] It is well-known that the oxidation state of a metal catalyst's surface strongly affects its catalytic behavior;[9] according to several reports in the literature, oxidized Pt,[10] Pd,[11] Rh,[12] and PtRh[13] surfaces are more efficient during the catalytic oxidation of CO than the pure metal surfaces. The reaction mechanisms of CO and NO oxidation are not well understood at the molecular level, however, and thus more information concerning the reactivity of catalytically active metals such as Pt is clearly needed.

The reactions of gas-phase metal clusters with small molecules represent a convenient, relatively simple means of modeling various catalytic processes.[14−20] For this reason, several groups have investigated the reactivity of platinum clusters with CO,[21] N_2, O_2, CO_2, and N_2O.[22] Koszinowski et al. studied the reactions of Pt_n^+ (n = 1−5) with H_2, O_2, NH_3, H_2O, CO_2, and N_2O,[23] as well as the reactions of $Pt_nCH_2^+$ (n = 1−5) with O_2, CH_4, NH_3, and H_2O.[24] Adlhart et al. examined the mechanisms involved in the dehydrogenation of alkanes by Pt_n^+ (n = 1−21) clusters.[25,26] Gruene et al. measured the C−O stretching frequency of $Pt_n(CO)^{+/0/-}$ (n = 3−22) by infrared multiple photon dissociation (IR-MPD) spectroscopy and found that CO binds in atop positions.[27] Ončák et al. reported the gas-phase reactivities of charged $Pt_2^{\pm}$ clusters with ammonia.[28]

Other groups have demonstrated the full catalytic cycle of CO oxidation; early experimental studies by Ervin and co-workers, for example, showed that platinum cluster anions, Pt_n^- (n = 3−6), efficiently catalyze the oxidation of CO to CO_2 by either N_2O or O_2 under thermal conditions.[29] During this catalytic cycle, intact clusters are regenerated and each step is exothermic and proceeds rapidly at thermal energies. Balaj et al. similarly studied CO oxidation by Pt_7^+ in mixtures of N_2O and CO,[30] and Koszinowski et al. investigated the chemical reactivity of cationic Pt_n^+ (n = 1−5) clusters with N_2O using Fourier transform ion cyclotron resonance (FT-ICR) mass spectrometry.[23] In addition, Balteanu et al. reported the rate constants for the reaction of cationic and anionic $Pt_n^{\pm}$ clusters (n = 1−24) with N_2O as measured by FT-ICR mass spectrometry.[31] They also investigated the conversion of CO and N_2O to CO_2 and N_2 on Pt_4^- and found that catalyst poisoning is observed when either $Pt_4O_4^-$ or $Pt_4(CO)_2^-$ is formed during the process.[32] More recently, Hermes et al. observed the infrared-driven CO oxidation reaction on isolated $Pt_nO_m^+$ (n = 3−7, m = 2,4) clusters[33] and found evidence of two competing reaction mechanisms consisting of CO desorption and CO oxidation, as indicated by CO_2 loss and the production of $Pt_nO_{m-1}^+$ cluster seen when using infrared multiple photon dissociation (IR-MPD) spectroscopy to monitor the clusters.

There have also been theoretical investigations of the mechanism by which CO oxidation occurs over Pt clusters. Rondinelli et al. analyzed the CO oxidation reaction paths when

Received: June 9, 2013
Revised: October 24, 2013
Published: October 24, 2013

dx.doi.org/10.1021/jp405707p | J. Phys. Chem. A 2013, 117, 12175−12183

using either atomic Rh^+ or Pt^+.[34] More recently, Lv et al. examined the catalytic mechanism of reactions of N_2O and CO over $Pt_4^{\pm}$ and found that Pt_4^- had a lower barrier for N_2O decomposition than Pt_4^+.[35]

Since the reactivity of neutral clusters differs from that of charged clusters, charge effects should be considered when assessing platinum catalysts.[36] Kaldor and co-workers researched the characteristics of neutral Pt clusters with regard to the chemisorption of H_2 and the dehydrogenation reactions of methane, benzene, and hexane.[37−39] Andersson and Rosén reported the catalytic oxidation of hydrogen on neutral platinum clusters (Pt_n; n = 7−30).[40] To the best of our knowledge, however, no studies concerning N_2O dissociation and CO oxidation on neutral Pt clusters have thus far been reported.

In this article, we report the study of chemical reactions of neutral platinum clusters with N_2O, together with the results of density functional theory (DFT) calculations. From the resulting data, absolute rate constants for the reactions of platinum and N_2O at room temperature were determined. The results of examinations of the reactions of platinum oxide clusters with CO are also reported.

EXPERIMENTAL AND COMPUTATIONAL DETAILS

Experimental Setup. Only a brief description of the experimental apparatus used in this study is provided here since this same apparatus has been described in detail in prior publications dealing with our work on rhodium[41] and nickel oxides[42] clusters. Platinum clusters were prepared by laser ablation. A Pt metal rod (Furuya Metal Co., Ltd., 99.99%) was used as the platinum source. The rod was constantly rotated and simultaneously moved in a sliding motion inside a stainless-steel block to maintain stable laser ablation conditions while being irradiated with focused 50 mJ laser pulses at 532 nm to generate plasma. The evaporated Pt atoms were cooled in a cylindrical channel (6 mm diameter) using He carrier gas (>99.99995%; stagnation pressure 0.9 MPa) ejected from the valve, and neutral and charged platinum clusters were formed as the plasma cooled. These clusters passed through the gas reaction cell (2 mm in diameter, 60 mm in length) as well as an extension tube (4 mm in diameter, 120 mm in length) with a resistive heater before expansion into the first vacuum chamber and were then introduced into a differentially pumped second chamber through a skimmer. Reactant gases (N_2O, CO) were injected into the reaction cell using a second solenoid pulsed valve, so as to study the chemical reactivity of the clusters. The reactant gases are diluted by He such that a constant total pressure of 1.1×10^5 Pa was maintained. The temperature of the extension tube was controlled within the range of 298−773 K using a resistive heater and was monitored by a thermocouple. Thermal equilibrium of the clusters was achieved by collisions with the He carrier gas well before expansion into the vacuum.

During the study of neutral cluster reactions, all charged clusters were removed from the beam using an electric field of +200 V applied to an electrode between the skimmer and acceleration electrodes. The remaining neutral clusters were photoionized by irradiation from a F_2 excimer laser (MPB PSX-100). The laser light was collimated to a 5 mm diameter beam, guided in dry N_2, and then introduced to the ionization region of the TOF-MS through a BaF_2 window. The typical laser pulse energy used for photoionization was <1500 μJ cm^{-2} and was measured using a power meter (Coherent J-10MB-LE) to avoid extensive multiphoton ionization.

In the mass analysis process, photoionized clusters gained kinetic energy of ∼3.5 keV in the acceleration region and were then steered and focused by a set of vertical and horizontal deflectors and an einzel lens. After traveling through a 1 m long field-free zone, the ions were reversed by a reflectron and detected using a Hamamatsu double-microchannel plate (MCP) detector. Signals from the detector were amplified with a 350 MHz preamplifier (Stanford SR445A) and digitized using an oscilloscope (LeCroy LT344L). Averaged TOF spectra (typically 1000 sweeps) were sent to a computer for analysis. The uncertainty associated with cluster abundance intensity measurements is estimated to be approximately ±20%. The mass resolution, $m/\Delta m$, exceeds 1500, which is sufficient to distinguish impurities, such as attached hydrogen atoms, that may affect cluster reactivity.

Computational Details. In order to elucidate differences in the reactivities of Pt_6O and Pt_nO (n > 6) clusters during reaction with N_2O, DFT calculations were performed using both the B3PW91[43] and B3LYP[44] exchange-correlation functionals. The B3PW91 functional satisfies the uniform electron gas (UEG) limit, which is considered to be important for pure metallic systems.[45,46] In contrast, although the B3LYP functional does not satisfy the UEG limit, it is well-known to properly describe molecules such as N_2O. In the present work, the results obtained by these functionals were compared with one another. The basis set used for nitrogen, oxygen, and platinum was the def2-SVP basis by Weigend and Ahlrichs,[47] whereas in the case of platinum, the 60 core electrons (1s−4f) were described using the scalar-relativistic effective core potential. All calculations were carried out using the Gaussian 09 program suite.[48] The charge distribution was determined by natural population analysis,[49] and we utilized the GRRM program[50−53] to find global minimum structures for Pt_6 and Pt_7 without relying on the intuitive selection of initial geometries since previous literature publications have shown that platinum clusters possess many local minimum structures.[54−58] Singlet, triplet, quintet, and septet spin states were taken into consideration. It was found that the singlet clusters generally showed severe spin contamination, suggesting that they were not pure singlet states, and hence, we neglect these states in the following discussion. In the case of oxidized Pt_nO (n = 6 and 7) clusters, their initial geometries were derived by attaching an oxygen atom to the most stable Pt_n isomers since they were generated in the reaction of the parent platinum clusters with N_2O in our experimental work. After optimizing the geometry of these clusters, the reactions of the most stable Pt_nO (n = 6 and 7) isomers with N_2O were investigated at all Pt atom sites. All the geometries shown in Figures 5−8 were identified as local minima or transition states through vibrational frequency analysis.

RESULTS

Figure 1 shows representative time-of-flight mass spectra of photoionized Pt_n clusters with and without addition of N_2O gas, from which it can be seen that Pt_n (n = 6−12) clusters were formed in the gas phase. A smooth distribution of cluster abundances is observed to have been generated under the applied conditions. According to the literature, the calculated ionization potentials of Pt_n clusters gradually increase with the cluster size (7.08, 7.16, and 7.45 eV for n = 6, 7, and 8, respectively).[55] As a result, we are able to ionize the gas-phase

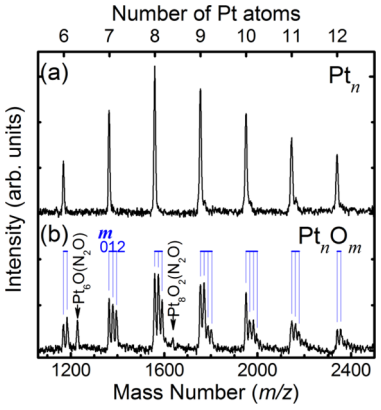

Figure 1. Mass spectra of neutral Pt_n clusters (a) with and (b) without the addition of 12.5% N_2O reactant gas (ca. 6×10^{17} cm^{-3}) at room temperature. The comb-like indicators show the m values of peaks corresponding to Pt_nO_m. Identical intensity scaling factors have been applied to each spectrum.

clusters by single photon absorption at a wavelength of 157 nm ($h\nu$ = 7.9 eV). It is apparent that newly formed oxidized Pt_nO_m clusters result from the successive oxygen-atom transfer reactions shown in eqs 1 and 2.

$$Pt_n + N_2O \rightarrow Pt_nO + N_2 \quad (1)$$

$$Pt_nO + N_2O \rightarrow Pt_nO_2 + N_2 \quad (2)$$

Similar reactions are known to occur with cationic and anionic platinum clusters.[23,31] Close analysis of the abundance of Pt_nO and the depletion of Pt_n following the reaction indicates that Pt_nO, Pt_nO_2, and $Pt_nO_m(N_2O)_k$ were formed in equivalent amounts to the quantity by which Pt_n was reduced. Hence, unlike the reaction of Pt_n with O_2,[23] any degradation (such as dissociation and fragmentation) of Pt_n clusters during the reaction with N_2O is considered to be negligible, likely because the release of stable N_2 molecules into the gas phase effectively removes excess energy generated by the reaction and therefore prevents the loss of Pt atoms associated with the formation of PtO_2.[23,30]

Figure 2 plots the relative intensities of the product clusters resulting from the reactions of Pt_n (n = 6 and 7) as a function of the number density of N_2O in the reaction cell. The relative intensity values were calculated as the ratio between the intensities of photoionized clusters following and prior to the reaction. The relative intensity of Pt_n can be seen to decrease monotonically, whereas the relative intensity of Pt_nO increases up to ~5×10^{17} cm^{-3} and then decreases with further increases in the number density of N_2O. In addition, both $Pt_6O(N_2O)$ and Pt_7O_2 begin to increase with further increases in the N_2O density. It should also be noted that the intensities of the pristine Pt_6 and Pt_7 clusters both converge on nonzero values.

Figure 3 shows the mass spectra of the products generated by reactions with N_2O and then heated to 298, 473, and 673 K in the extension tube. It is clearly seen that $Pt_6O(N_2O)$ and the other N_2O adducts which were observed at 298 K are completely absent at a temperature of 473 K. Moreover, the sole observed oxide for Pt_6 is Pt_6O. Figure 3 also demonstrates an overall trend whereby the quantity of oxygen atoms in the metal oxide clusters is decreased by postheating.[42] The observation that no Pt_nO_2 clusters remain intact upon heating to 673 K indicates that either O_2 molecule or PtO_2 moieties dissociate from the Pt_6O_2 clusters during the heating process.

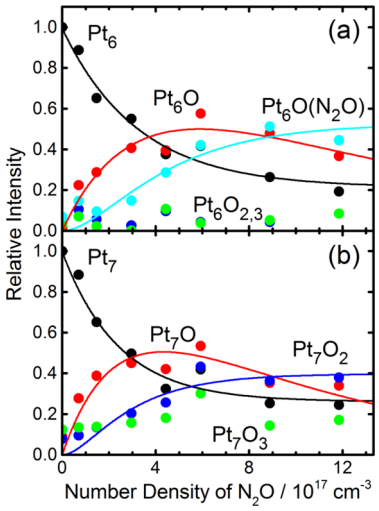

Figure 2. Relative intensity of (a) Pt_6 and (b) Pt_7 and their respective reaction products as a function of the number density of N_2O gas in the gas reaction cell at room temperature. Filled black, red, cyan, blue, and green circles indicates Pt_n, Pt_nO, $Pt_6O(N_2O)$, Pt_nO_2, and Pt_nO_3, respectively. A number density of 5×10^{17} cm^{-3} corresponds to ca. 80 Torr. The overlaid lines represent the least-squares fits generated using eqs 6 through 8.

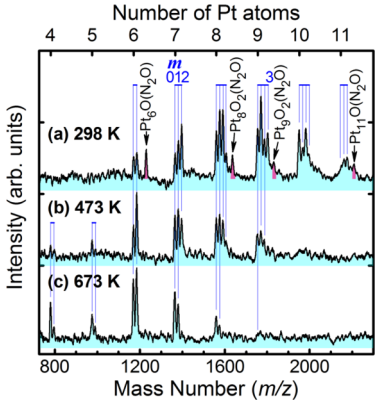

Figure 3. Mass spectra of neutral Pt_n clusters with 0.5% N_2O at (a) 298 K, (b) 473 K, and (c) 673 K. The comb-like indicators show the m values of peaks corresponding to Pt_nO_m. Identical intensity scaling factors have been applied to each spectrum. The $Pt_nO_m(N_2O)$ clusters indicated by arrows were diminished by heating prior to expansion in the vacuum.

PtO_2 is a volatile compound, which is known to form when Pt is subjected to high temperatures under an oxidizing atmosphere.[59−63] Hannevold et al. reported the chemical vapor transport of Pt and Rh using oxygen as the transport agent according to the reaction equation $M(s) + O_2(g) \rightarrow MO_2(g)$, where M = Pt or Rh.[62] Taking this into account, it is likely that Pt_nO_m clusters in which $m > 2$ decompose into either $Pt_{n-1}O_{m-2}$ and a volatile PtO_2 molecule or Pt_nO_{m-2} and an O_2 molecule. In contrast, clusters with the general formula Pt_nO remain unaffected by heating since emission of a single oxygen atom is energetically unfavorable.

DISCUSSIONS

Sequential Reactions of Pt_n with N_2O. As can be deduced from Figures 1 and 2, a single oxygen atom transfers from N_2O to a Pt cluster during the initial gas-phase reaction of these two compounds, as per eq 1. Sequential oxygen transfer

dx.doi.org/10.1021/jp405707p | J. Phys. Chem. A 2013, 117, 12175−12183

reactions then occur, generating Pt_nO_2 from Pt_nO as shown in eq 2. The degree to which these reactions occur, however, is strongly size-dependent. The sequential reaction of Pt_7 and N_2O, for example, produces Pt_7O_2, whereas the reaction of Pt_6 with N_2O results in the formation of $Pt_6O(N_2O)$ rather than Pt_6O_2. $Pt_6O(N_2O)$ is considered to be composed of Pt_6O and a weakly attached N_2O molecule because N_2O was found to be released from $Pt_6O(N_2O)$ upon postheating. If a second oxygen atom had been transferred from N_2O to Pt_6O, we would expect to observe Pt_6O_2 in the mass spectrum. It is worth noting that, during the reaction of cationic clusters, the absence of $Pt_6O_2^+$ and the formation of $Pt_6O(N_2O)^+$ is also observed (see Figure S1, Supporting Information), whereas $Pt_6O_2^+$ is known to form readily by the reaction of Pt_n^+ clusters and O_2 gas.[33] The lack of $Pt_6O_2^+$ following the reaction with N_2O is therefore the result of differences in reaction kinetics. Interestingly, Balaj et al. observed the formation of $Pt_6O_2^+$ from the reaction between Pt_6^+ and N_2O when using a 1:6 ratio of CO to N_2O in an ICR cell.[30] It seems probable that the coexistence of N_2O and CO may therefore allow the reaction channel that produces $Pt_6O_2^+$.

In order to quantitatively assess these oxygen transfer reactions, absolute rate constants were obtained from the rate equations. Assuming that the reagent gas is in sufficient excess, the pseudo-first order kinetics expression for cluster depletion may be expressed as

$$\ln \frac{I}{I_0} = -kP_{N_2O}\tau \tag{3}$$

where I and I_0 are mass spectral peak areas in the presence and absence of the reagent gas, k is the absolute rate constant, P_{N_2O} is the reagent partial pressure in the gas reaction cell, and τ is the reactant contact time. In order to estimate the number density in the reaction cell, the reaction of atomic V^+ with gas phase CO prepared under identical experimental conditions was observed as a reference. The rate constant for the reaction of V^+ with CO is known to be $(7 \pm 2) \times 10^{-14}$ cm^3 s^{-1},[64] which allows the product of P_{N_2O} and τ to be calculated. The residence time of platinum clusters in the reaction gas cell, which equates to τ, was estimated to be approximately 70 μs, and so the reactant gas number density was calculated to be $\sim 10^{17}$ molecules cm^{-3}.

As shown in Figure 2, the peak intensities of unreacted Pt_6 and Pt_7 clusters reach nonzero equilibrium values, and as such, the reverse N_2O association reaction should be taken into account. The reaction given as eq 1 can be broken down into more elementary steps consisting of the initial N_2O association followed by the subsequent loss of N_2, as in eq 4.

$$Pt_n + N_2O \underset{k_b}{\overset{k_f}{\rightleftarrows}} Pt_n(N_2O)^{\ddagger} \overset{k_p}{\rightarrow} Pt_nO + N_2 \tag{4}$$

The rate constants associated with the first reaction in the forward and reverse directions are termed k_f and k_b, and k_p is the rate constant for the N_2 detachment reaction. Assuming that the N_2O dissociation reaction is slow, $k_p \ll k_f$ and k_b, and the sum of the rate constants $(k_f + k_b)$ can be obtained using the following equation:

$$\frac{I - I_e}{I_0 - I_e} = A\, e^{-(k_f + k_b)[N_2O]t} \tag{5}$$

where A is an arbitrary constant and I_e is the mass spectral peak area at equilibrium. By fitting the rate eqs 6 through 8 below for the sequential chemical reactions to the obtained data, we were able to calculate the rate constants k_1 and k_2 for reactions 1 and 2, respectively.

$$\frac{I_{Pt_n}}{I_{Pt_n,0}} = A_e + A\, e^{-k_1[N_2O]t} \tag{6}$$

$$\frac{I_{Pt_nO}}{I_{Pt_nO,0}} = A\frac{k_1}{k_2 - k_1}(e^{-k_1[N_2O]t} - e^{-k_2[N_2O]t}) \tag{7}$$

$$\frac{I_{Pt_nO_2}}{I_{Pt_nO_2,0}} = A\left(1 + \frac{k_1}{k_2 - k_1}e^{-k_2[N_2O]t} - \frac{k_2}{k_2 - k_1}e^{-k_1[N_2O]t}\right) \tag{8}$$

Figure 4 summarizes the variations in the absolute rate constants k_1 and k_2 with cluster size. For Pt_6, the rate constant

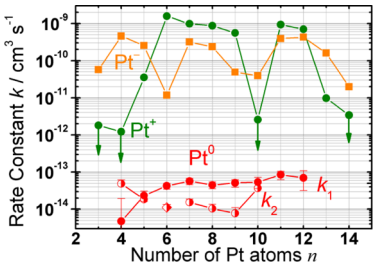

Figure 4. Variations with cluster size of the absolute rate constants k_1 and k_2 for the oxidation reaction of neutral Pt_n clusters with N_2O (red filled and half-filled symbols, respectively) on a semilogarithmic scale. Absolute rate constants for the attachment reaction of neutral Pt_6O clusters and N_2O molecules are plotted as red diamonds, while literature data for charged $Pt_n^{\pm}$ clusters are shown in green and orange.[31]

for the formation of $Pt_6O(N_2O)$ is plotted instead of k_2. As can be seen from these data, the rate constants range from 10^{-14} to 10^{-13} cm^3 s^{-1} and do not vary significantly with cluster size (k_2 for Pt_6 was not observed). The size dependence of k_1 for the reaction of neutral platinum clusters with N_2O bears a qualitative resemblance to the trend observed for reactions with O_2 as reported by Andersson et al.[40] The values of k_1 plotted for the cationic platinum clusters are almost 3 orders of magnitude greater than those of the neutral clusters over the entire size range studied. This difference is very large compared to variations associated with the other reaction. For instance, the reaction between $Nb^{-/0/+}$ clusters and D_2 molecules, in which the reactivity of ions is generally within a factor of 2.5 times that of the corresponding neutral clusters.[65] Koszinowski et al. determined the bimolecular rate constants for the reaction of $Pt_{3,5}O_m^+$ clusters and N_2O, and found that rate constants for the addition reaction are larger when $m = 1$ compared to $m = 0$.[23] In our study, however, no significant enhancement of k_2 was found with cluster size.

Formation of $Pt_6O(N_2O)$ and Other $Pt_nO_m(N_2O)_k$. As shown in Figures 1 and 2, Pt_6 was oxidized by the reaction with N_2O just as readily as the other neutral platinum clusters. However, as noted earlier, Pt_6O_2 was not generated by the reaction of Pt_6O with N_2O, and in addition, the species $Pt_6O(N_2O)$, in which N_2O is attached to the cluster, was observed in the mass spectrum obtained under the higher N_2O gas density condition. Other similar N_2O adducts including $Pt_8O_2(N_2O)$, $Pt_9O_2(N_2O)$, and $Pt_{11}O(N_2O)$ were also observed (see Figure 3).

dx.doi.org/10.1021/jp405707p | J. Phys. Chem. A 2013, 117, 12175−12183

In general, only a limited number of neutral $Pt_nO_m(N_2O)_k$ species were observed when applying our particular experimental conditions, consisting of $Pt_6O(N_2O)$, $Pt_8O_2(N_2O)$, $Pt_9O_2(N_2O)$, and $Pt_{11}O(N_2O)$. It is interesting that N_2O adducts were formed only in the case of the most or the second most highly oxidized Pt_n clusters. In contrast, during the reactions of the cationic clusters (see Figure S1, Supporting Information) N_2O adducts were formed with every size of Pt_n^+ investigated, generating $Pt_3(N_2O)_{1-4}^+$, $Pt_4(N_2O)_{1-4}^+$, $Pt_5(N_2O)_{1-4}^+$, $Pt_6O(N_2O)_{1-4}^+$, $Pt_7O_2(N_2O)_{1-3}^+$, $Pt_8O_2(N_2O)_{1-3}^+$, $Pt_9O_2(N_2O)_{1-3}^+$, and $Pt_{10}O_2(N_2O)_{1-2}^+$, along with small amounts of $Pt_3O(N_2O)_{1-3}^+$ and $Pt_3O_2(N_2O)_{1-3}^+$. Compared to the neutral clusters reacted at the same N_2O number density, the cationic clusters also generated much larger quantities of N_2O adducts. When reacting $Pt_n^{+/0}$ clusters, it was observed that the adduct intensity decreased monotonically as the N_2O number increased. The difference between the abundance of N_2O adducts generated by cationic and neutral clusters can be explained by the greater energy associated with the binding of N_2O with cationic Pt_n^+ as compared to neutral Pt_n clusters. The charge−dipole interaction involved in binding to the charged clusters is much larger than the induced charge dipole interaction of the neutral clusters. In essence, the adduct species can be considered as the result of solvation of the core Pt_n^+ or Pt_nO^+ clusters by N_2O molecules. Hence, the simple attachment and decomposition of N_2O seem to be competing processes in some cationic and neutral clusters.

$$Pt_6O + N_2O \longrightarrow Pt_6O(N_2O) \nrightarrow Pt_6O_2 + N_2 \quad (9)$$

These results suggest that most energized intermediate complexes, such as $Pt_n(N_2O)^{\ddagger}$, are unstable due to the relatively low binding energy and hence are not efficiently stabilized by collisions with the He buffer gas but instead react to produce Pt_nO, and consequently, intermediate complexes such as $Pt_6(N_2O)$ are not observed. Even so, some N_2O adducts of oxidized clusters, such as $Pt_6O(N_2O)$, can persist. Possible reasons for the increased stability and persistence of the neutral adducts may include the polarization of the Pt−O bond and the high activation energy barrier associated with N_2O decomposition. We will discuss this issue in more detail on a theoretical basis in the following section.

Reaction Mechanism of Pt Clusters with N_2O. On the basis of the results of DFT calculations, we identified either 39 or 37 possible isomers of the Pt_6 cluster, using the B3LYP and B3PW91 functionals, respectively. Only the lowest lying isomers (within 0.3 eV from the most stable isomer) are shown in Figure 5. Results regarding these isomers suggest the existence of a general propensity for the low-lying clusters to have compact three-dimensional structures. Although the B3LYP functional also predicts planar isomers, such as the quintet Q_{II} and the triplet T_{II}, these are not found to be stable when calculated using the B3PW91 functional, which provides a better description of pure metal systems than the B3LYP functional; this is because the B3PW91 functional fulfills the uniform electron gas (UEG) limit, which is considered to be important for pure metallic systems. As an example, the B3PW91 functional gives the correct global minimum structure for pure metallic Na_4, whereas the B3LYP functional provides an incorrect structure.

Both of the functionals predict a prismatic structure (S_I, S'_I) with the septet spin state as the global minimum. We subsequently placed an oxygen atom at possible sites on the

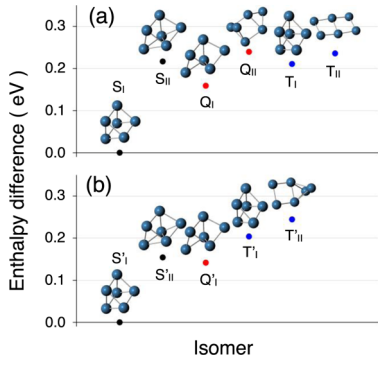

Figure 5. Low-lying isomers of Pt_6 clusters, within 0.3 eV from the most stable structure, as obtained by (a) B3LYP and (b) B3PW91 exchange-correlation functionals. The symbols S, Q, and T indicate septet, quintet, and triplet spin multiplicities for clusters, respectively.

stable isomers of Pt_6 and calculated the energies of the resulting structures using the B3LYP functional. These calculations found that an isomer with the oxygen atom adsorbed at the on-top site of a platinum atom in the S_I cluster is the most stable form, as shown in Figure 6. Note that the oxygen atom adsorption energies are almost identical for all the platinum atoms in the cluster.

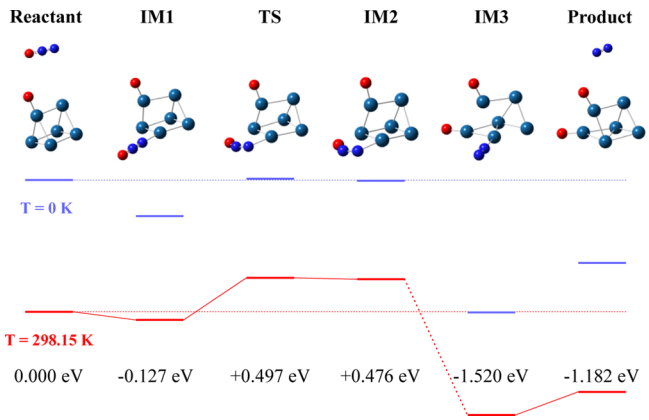

Figure 6. Gibbs free energy profile along the reaction $Pt_6O + N_2O \rightarrow Pt_6O_2 + N_2$. Pt, cyan spheres; N, blue spheres; O, red spheres.

Figure 6 shows the Gibbs free energy profile for the reaction $Pt_6O + N_2O \rightarrow Pt_6O_2 + N_2$, as calculated using the B3LYP functional. The applicability of this functional when describing this type of reaction has been established by Lv et al.[35] For simplicity, we show the energy profile only for the isomer having the lowest energy. In the case of the IM1 isomer shown in Figure 6, N_2O is weakly bound to the Pt_6O cluster with the terminal nitrogen atom pointing to one of the Pt atoms to which the first oxygen atom is not attached. The binding energy was calculated to be ∼0.13 eV at 298.15 K, which is a typical value for physisorption and consistent with the propensity for N_2O to be readily released from $Pt_6O(N_2O)$ by heating. We investigated the relative stability of the adducts in which N_2O is attached to the other Pt atoms and confirmed that the IM1 isomer in Figure 6 is the most stable among them. In the IM1 isomer, the N_2O-binding Pt is positioned primarily along the line of the molecular axis. To initiate the oxygen transfer reaction, however, the N_2O molecule is required to bend, which causes an increase in free energy. After the complex passes through this transition state, the oxygen atom in N_2O binds to a

dx.doi.org/10.1021/jp405707p | J. Phys. Chem. A 2013, 117, 12175−12183

Pt atom and the bond between N_2 and O ruptures. The energy of the transition state leading to the formation of Pt_6O_2 is so high ($\sim 19\ k_BT$) that the reaction is not expected to occur at 298.15 K. In contrast, the energy of the transition state is nearly equal to the energy of the reactant at 0 K, and hence, Pt_6O_2 is predicted to form at lower temperatures. In other words, the lower entropy associated with the transition state due to the reduced degree of freedom is the cause of the higher reaction barrier.

The same calculation was performed for Pt_7O, which reacts readily with N_2O to form Pt_7O_2. Figure 7 shows the lowest

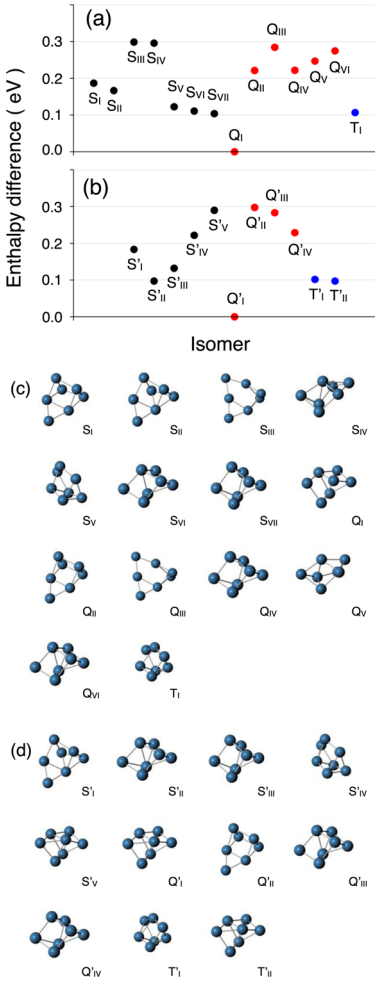

Figure 7. Relative energies of low-lying isomers of Pt_7 clusters, within 0.3 eV of the most stable isomer, obtained by (a) B3LYP and (b) B3PW91 exchange-correlation functionals, as well as corresponding geometries obtained with (c) B3LYP and (d) B3PW91 functionals. The symbols S, Q, and T indicate septet, quintet, and triplet spin multiplicities for clusters, respectively.

lying Pt_7 clusters, within 0.3 eV of the most stable isomer. The global minima are the quintet Q_I and Q'_I isomers, each of which has essentially the same electronic and geometric structure. We noted that, compared to the Pt_6 clusters, there are many isomers of Pt_7 in the same energy range. Moreover, some isomers include planar substructures such as S_I, S_{II}, S_{III}, Q_{II}, and Q_{III}, as shown in Figure 7a (B3LYP), and S'_I and Q'_{II}, as shown in Figure 7b (B3PW91). Attaching an oxygen atom to the various possible sites of the most stable isomer of Pt_7, the quintet Q_{II} cluster, which has planar triangle substructures, was found to yield the most stable cluster.

We subsequently investigated the reaction mechanism of Pt_7O derived from the Q_{II} isomer, as shown in Figure 8. The

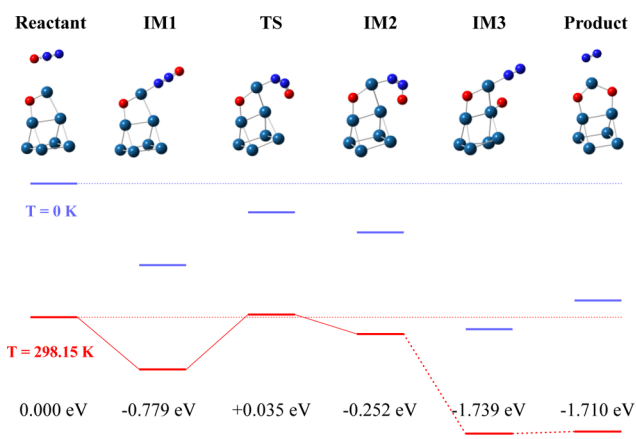

Figure 8. Free energy profile along the reaction $Pt_7O + N_2O \rightarrow Pt_7O_2 + N_2$. Pt, cyan spheres; N, blue spheres; O, red spheres.

first oxygen atom attaches in a bidentate fashion at the edge of a planar triangle substructure, and this oxygen atom plays an important role with regard to stabilizing the subsequent adsorption of N_2O. As shown for the IM1 isomer of Figure 8, the N_2O attaches with the terminal nitrogen atom pointing to one of the Pt atoms to which the first oxygen atom has attached. The resultant O−Pt−N−N−O arrangement is almost linear, and the charge distribution of this moiety is O(−0.66)−Pt(+0.32)−N(−0.15)−N(+0.48)−O(−0.30). As the result of the strong electrostatic interactions resulting from this linear configuration, the binding energy of N_2O is increased to ~0.78 eV, which is a value typical of chemisorption and is much higher than the binding energy obtained when using the Pt_6O cluster. The barrier height for Pt_7O is below 0.035 eV at 298.15 K, and so there is a reasonable probability that the reaction intermediate will have sufficient energy to pass through the transition state. This explanation is consistent with the experimental observation that Pt_nO clusters generally exhibit higher levels of reactivity with N_2O than Pt_n clusters.[23] Lv et al. have ascribed the high reactivity of planar Pt_4^- to the electron transfer from Pt_4^- to N_2O.[35] In contrast, the total overall charge on N_2O in the transition state is nearly equal to zero in our neutral system, and therefore, it is highly likely that, for the neutral clusters, the strong binding of N_2O is assisted by the preadsorbed oxygen purely as a result of the geometrical effect of the planar triangle substructure enhancing the reactivity of Pt_7O. For larger clusters, there would be many isomers having such planar substructures in the low-energy region, which would enhance the reactivity of neutral clusters.

Comparison of the N_2O Reactivities of Neutral Pt and Rh Clusters. In our previous study, we observed gas-phase catalytic reactions involving the reduction of N_2O by neutral rhodium clusters, Rh_n (n = 10−28).[41] Sequential oxygen transfer reactions according to the formula $Rh_nO_{m-1} + N_2O \rightarrow Rh_nO_m + N_2$ (m = 1, 2, 3, etc.) were demonstrated, and the rate constant for each reaction step was determined as a function of the cluster size. In the present study, we attempted to ascertain whether neutral Pt_n (n = 4−12) clusters exhibit the same level of reactivity as Rh_n toward N_2O. As shown in Figure 4, however, the rate constants for Pt_n oxygen transfer reactions 1

dx.doi.org/10.1021/jp405707p | J. Phys. Chem. A 2013, 117, 12175−12183

and 2 range from 4×10^{-14} to 2×10^{-13} cm^3 s^{-1} (except in the case of Pt_4) and thus are lower than the rate constants previously determined for Rh_n (1×10^{-13} to 1×10^{-12} cm^3 s^{-1} for n = 10−28) by 1 order of magnitude.

In this work, the reaction products Pt_nO and Pt_nO_2 were observed when the density of N_2O was raised to a sufficiently high value. More highly oxidized clusters, however, such as Pt_nO_m (m > 3 or 4), were not observed even when the density of N_2O was further increased. Instead, various N_2O-attached clusters, including $Pt_6O(N_2O)$, $Pt_8O_2(N_2O)$, $Pt_9O_2(N_2O)$, and $Pt_{11}O(N_2O)$, appeared in the mass spectra. Since the clusters were only observed following photoionization, it is possible that the more highly oxidized clusters were not ionized by the F_2 laser. However, the total ion intensities did not change appreciably when the N_2O gas density was increased, which indicates that additional oxygen transfer reactions do not proceed to any significant extent at higher N_2O density levels. In summary, the oxygen transfer reactions that occur in the presence of Pt_n clusters are different from those of Rh_n. Although Rh_nO_m products with m as high as 6 were observed following the oxidation reactions of Rh_n, a limit of 3 oxygen atoms could be transferred from N_2O to Pt_n. As shown by the DFT calculations, Pt clusters require the presence of special substructures to stabilize the transition state necessary for N_2O reduction, which implies that these clusters will typically be inactive with respect to the reaction.

Coadsorption of O and CO on Neutral Pt Clusters. We attempted to determine if catalytic reactions involving the reduction of N_2O and the concurrent oxidation of CO actually occur in the presence of neutral platinum clusters, Pt_n. To this end, we prepared Pt_nO_m in the cluster source by mixing N_2O, CO, or a combination of N_2O and CO with the He carrier gas. Figure 9 shows the mass spectra of the photoionized neutral

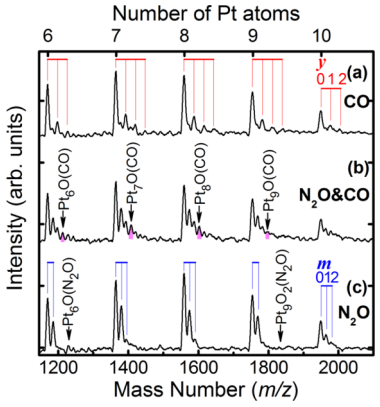

Figure 9. Mass spectra of the reaction of neutral Pt_n clusters with (a) 0.25% CO (ca. 1.2×10^{16} cm^{-3}), (b) 25% N_2O, and 0.25% CO, and (c) 25% N_2O (ca. 1.2×10^{18} cm^{-3}) at 373 K. Comb-like indicators show the y and m values of $Pt_n(CO)_y$ and Pt_nO_m. Peaks corresponding to $Pt_nO(CO)$ are indicated by arrows.

clusters after reaction with these various gases. Following reaction solely with CO, peaks corresponding to $Pt_n(CO)_y$ (y = 0 to 2 or 3) were observed, as seen in Figure 9b. The maximum number of attached CO molecules seen here is slightly higher than in the species $Pt_6(CO)_2$ and $Pt_7(CO)_1$ previously reported by Cox et al.[66] In contrast, reaction with N_2O generated Pt_nO_m (m = 0, 1), as shown in Figure 9c. From Figure 9b, it is evident that Pt_nO_mCO was formed as a consequence of the depletion of Pt_nO_m by the reaction shown as eq 10.

$$Pt_nO_m + CO \rightarrow Pt_nO_mCO \quad (10)$$

This reaction is exothermic and the energy that it generates is absorbed by collisions with the surrounding He atoms. A similar reaction scheme is proposed in the case of cationic $Pt_nO_m^+$ clusters and is summarized in Figure S2, Supporting Information.

When reacting Rh clusters, we observed the loss of oxygen atoms that had been attached to the Rh clusters following reaction with CO, such that the mass peaks due to Rh_nO_m clusters distributed around m = 1−6 prior to the reaction were shifted to m = 0−3 after the reaction.[41] This loss of oxygen atoms indicates that the reaction $Rh_nO_m + CO \rightarrow Rh_nO_{m-1} + CO_2$ proceeds efficiently in the gas phase. When reacting the less oxidized clusters with the general formula Rh_nO_m ($m \leq 3$), however, only the attachment of CO was observed to form Rh_nO_mCO. These findings lead to the conclusion that rhodium clusters operate as more efficient catalysts when they are oxidized and are less efficient when they are not oxidized or less fully oxidized. It is likely that the O−Rh_n binding energy may decrease with increases in the oxygen number, causing oxygen transfer to occur more readily during reactions of the more highly oxidized Rh_n clusters.

In this work, as discussed above, the oxidation of Pt clusters by N_2O was observed to proceed to a lesser extent. The loss of oxygen atoms from Pt_nO_m as a consequence of reaction with CO was unremarkable, probably because oxygen atoms strongly bind to Pt_n when the number of oxygen atoms is m = 1 or 2. In conventional catalytic reactions, heat must be applied to the clusters so that coadsorbed oxygen atoms and CO molecules desorb as CO_2. This is problematic, however, since the likelihood of an oxygen transfer reaction between N_2O and Pt_n decreases when the cluster temperature is increased by heating because the energy barrier of the transfer reaction is also increased. As a result, we consider that neutral Pt_n clusters are less efficient at promoting the catalytic reduction of N_2O and the oxidation of CO than the neutral rhodium clusters, Rh_n. This phenomenon has been recognized previously and has been referred to as the poisoning effect of CO on Pt catalysts.[30]

CONCLUSIONS

We studied the reactions of neutral Pt_n (n = 4−12) clusters with N_2O and CO in the gas phase. During the reaction of the clusters with N_2O, oxygen transfer reactions that may be summarized by the formula $Pt_nO_{m-1} + N_2O \rightarrow Pt_nO_m + N_2$ (m = 1 and 2) are predominant. Additional oxygen transfer reactions resulting in Pt_nO_m ($m \geq 4$) were not observed, even when the gas density of N_2O was raised to a level that should have been sufficient to promote such reactions. We also observed that Pt_6O is totally inactive toward N_2O under our experimental conditions because of the reaction barrier between $Pt_6O(N_2O)$ and $Pt_6O_2 + N_2$, a finding that was confirmed by density functional theory calculations. The absolute rate constants associated with the oxidation reactions, k_1 and k_2, range from 10^{-13} to 10^{-12} cm^3 s^{-1} and do not vary significantly with the cluster size, with the exception of the k_2 constant for Pt_6, which is not observable. The k_1 values of neutral clusters were found to be 3 times lower than the corresponding rate constants of ionic clusters.

The possibility of applying neutral Pt_n species to the catalytic reduction of N_2O, as well as to the oxidation of CO, was also examined. It was found that Pt_n did not show any significant catalytic abilities but rather that O and CO coadsorb to Pt_n.

dx.doi.org/10.1021/jp405707p | J. Phys. Chem. A 2013, 117, 12175−12183

The desorption of CO_2 from the coadsorbed clusters was not clearly identified from the results of mass spectrometry. This is in contrast to the behavior of Rh_n clusters upon exposure to CO; CO_2 desorption has been observed in cases where more than 3 oxygen atoms are bound to the Rh_n, whereas the coadsorption of O and CO takes place when less than 2 oxygen atoms bind to Rh_n. The similarity between the coadsorption behaviors of Rh_n and Pt_n suggests that the oxygen atom binds rather strongly to Pt_n, and hence, the desorption of CO_2 is hindered. The above findings lead us to conclude that neutral platinum clusters, Pt_n (n = 4−12), do not exhibit any remarkable catalytic activity with regard to reactions with N_2O or CO.

■ ASSOCIATED CONTENT

Supporting Information

Mass spectra of cationic Pt_n^+ clusters acquired with or without N_2O, CO, or a mixture of N_2O and CO at room temperature. This material is available free of charge via the Internet at http://pubs.acs.org.

■ AUTHOR INFORMATION

Corresponding Author

*(F.M.) E-mail: mafune@cluster.c.u-tokyo.ac.jp. Tel: +81 3 5454 6597.

Present Address

†(T.Y.) The Open University of Japan, Mihama-ku, Chiba, Japan.

Notes

The authors declare no competing financial interest.

■ ACKNOWLEDGMENTS

This work was supported by JSPS KAKENHI Grant Numbers 25248004 and 24550010, and additional funding for cluster research was provided by the Genesis Research Institute, Inc.

■ REFERENCES

(1) Zaera, F.; Somorjai, G. Hydrogenation of Ethylene over Platinum (111) Single-Crystal Surfaces. *J. Am. Chem. Soc.* **1984**, *106*, 2288−2293.

(2) Silveston, P. L. Automotive Exhaust Catalysis under Periodic Operation. *Catal. Today* **1995**, *25*, 175−195.

(3) Takahashi, N.; Shinjoh, H.; Iijima, T.; Suzuki, T.; Yamazaki, K.; Yokota, K.; Suzuki, H.; Miyoshi, N.; Matsumoto, S.; Tanizawa, T. The New Concept 3-Way Catalyst for Automotive Lean-Burn Engine: NO_x Storage and Reduction Catalyst. *Catal. Today* **1996**, *27*, 63−69.

(4) Koltsakis, G. C.; Stamatelos, A. M. Catalytic Automotive Exhaust Aftertreatment. *Prog. Energy Combust. Sci.* **1997**, *23*, 1−39.

(5) Granger, P.; Leclercq, G. Reduction of N_2O by CO over Ceria-Modified Three-Way Pt-Rh Catalysts: Kinetic Aspects. *J. Phys. Chem. C* **2007**, *111*, 9905−9913.

(6) Bowker, M. Automotive Catalysis Studied by Surface Science. *Chem. Soc. Rev.* **2008**, *37*, 2204−2211.

(7) Ervin, K. M.; Ho, J. Lineberger, Electronic and Vibrational Structure of Transition Metal Trimers: Photoelectron Spectra of Ni, Pd, and Pt. W. *J. Chem. Phys.* **1988**, *89*, 4514−4521.

(8) Harding, D. J.; Kerpal, C.; Rayner, D. M. Fielicke, Communication: The Structures of Small Cationic Gas-Phase Platinum Clusters. *J. Chem. Phys.* **2012**, *136*, 211103.

(9) Mittendorfer, F.; Franz, T.; Klikovits, J.; Schmid, M.; Merte, L. R.; Zaman, S. S.; Varga, P.; Westerstrom, R.; Resta, A.; Andersen, J. N.; Gustafson, J.; Lundgren, E. Oxygen-Stabilized Rh Adatoms: 0D Oxides on a Vicinal Surface. *J. Phys. Chem. Lett.* **2011**, *2*, 2747−2751.

(10) Ackermann, M. D.; Pedersen, T. M.; Hendriksen, B. L. M.; Robach, O.; Bobaru, S. C.; Popa, I.; Quiros, C.; Kim, H.; Hammer, B.; Ferrer, S. Structure and Reactivity of Surface Oxides on Pt (110) during Catalytic CO Oxidation. *Phys. Rev. Lett.* **2005**, *95*, 255505.

(11) van Rijn, R.; Balmes, O.; Felici, R.; Gustafson, J.; Wermeille, D.; Westerström, R.; Lundgren, E.; Frenken, J. W. Comment on CO Oxidation on Pt-Group Metals from Ultrahigh Vacuum to Near Atmospheric Pressures. 2. Palladium and Platinum. *J. Phys. Chem. C* **2010**, *114*, 6875−6876.

(12) Gustafson, J.; Westerstrom, R.; Balmes, O.; Resta, A.; van Rijn, R.; Torrelles, X.; Herbschleb, C. T.; Frenken, J. W. M.; Lundgren, E. Catalytic Activity of the Rh Surface Oxide: CO Oxidation over Rh (111) under Realistic Conditions. *J. Phys. Chem. C* **2010**, *114*, 4580−4583.

(13) Westerström, R.; Wang, J. G.; Ackermann, M. D.; Gustafson, J.; Resta, A.; Mikkelsen, A.; Andersen, J. N.; Lundgren, E.; Balmes, O.; Torrelles, X. Structure and Reactivity of a Model Catalyst Alloy under Realistic Conditions. *J. Phys.: Condens. Matter* **2008**, *20*, 184018.

(14) Bernhardt, T. M.; Heiz, U.; Landman, U. Chemical and Catalytic Properties of Size-Selected Free and Supported Clusters. In *Nanocatalysis*; Heiz, U., Landman, U., Eds.; Springer: Berlin, Germany, 2007; pp 1−191.

(15) Brönstrup, M.; Schröder, D.; Kretzschmar, I.; Schwarz, H.; Harvey, J. N. Platinum Dioxide Cation: Easy to Generate Experimentally but Difficult to Describe Theoretically. *J. Am. Chem. Soc.* **2001**, *123*, 142−147.

(16) Lang, S. M.; Bernhardt, T. M. Gas Phase Metal Cluster Model Systems for Heterogeneous Catalysis. *Phys. Chem. Chem. Phys.* **2012**, *14*, 9255−9269.

(17) Yin, S.; Bernstein, E. R. Gas Phase Chemistry of Neutral Metal Clusters: Distribution, Reactivity and Catalysis. *Int. J. Mass Spectrom.* **2012**, *321−322*, 49−65.

(18) Bernhardt, T. M. Gas-Phase Kinetics and Catalytic Reactions of Small Silver and Gold Clusters. *Int. J. Mass Spectrom.* **2005**, *243*, 1−29.

(19) Bernhardt, T. M.; Socaciu-Siebert, L. D.; Hagen, J.; Wöste, L. Size and Composition Dependence in CO Oxidation Reaction on Small Free Gold, Silver, and Binary Silver−Gold Cluster Anions. *Appl. Catal., A* **2005**, *291*, 170−178.

(20) Bozovic, A.; Feil, S.; Koyanagi, G. K.; Viggiano, A. A.; Zhang, X.; Schlangen, M.; Schwarz, H.; Bohme, D. K. Conversion of Methane to Methanol: Nickel, Palladium, and Platinum (d^9) Cations as Catalysts for the Oxidation of Methane by Ozone at Room Temperature. *Chem.—Eur. J.* **2010**, *16*, 11605−11610.

(21) Ren, X. L.; Hintz, P. A.; Ervin, K. M. Chemisorption of Carbon-Monoxide on Platinum Cluster Anions. *J. Chem. Phys.* **1993**, *99*, 3575−3587.

(22) Hintz, P. A.; Ervin, K. M. Chemisorption and Oxidation Reactions of Nickel Group Cluster Anions with N_2, O_2, CO_2, and N_2O. *J. Chem. Phys.* **1995**, *103*, 7897−7906.

(23) Koszinowski, K.; Schroder, D.; Schwarz, H. Reactivity of Small Cationic Platinum Clusters. *J. Phys. Chem. A* **2003**, *107*, 4999−5006.

(24) Koszinowski, K.; Schroder, D.; Schwarz, H. Reactions of Platinum−Carbene Clusters $Pt_nCH_2^+$ (n = 1−5) with O_2, CH_4, NH_3, and H_2O: Coupling Processes Versus Carbide Formation. *Organometallics* **2003**, *22*, 3809−3819.

(25) Adlhart, C.; Uggerud, E. Reactions of Platinum Clusters $Pt_n^{\pm}$, n = 1−21, with CH_4: To React or Not to React. *Chem. Commun.* **2006**, 2581−2582.

(26) Adlhart, C.; Uggerud, E. Mechanisms for the Dehydrogenation of Alkanes on Platinum: Insights Gained from the Reactivity of Gaseous Cluster Cations, Pt_n^+ n = 1−21. *Chem.—Eur. J.* **2007**, *13*, 6883−6890.

(27) Gruene, P.; Fielicke, A.; Meijer, G.; Rayner, D. M. The Adsorption of CO on Group 10 (Ni, Pd, Pt) Transition-Metal Clusters. *Phys. Chem. Chem. Phys.* **2008**, *10*, 6144−6149.

(28) Ončak, M.; Cao, Y.; Beyer, M. K.; Zahradnik, R.; Schwarz, H. Gas-Phase Reactivities of Charged Platinum Dimers with Ammonia: A Combined Experimental/Theoretical Study. *Chem. Phys. Lett.* **2008**, *450*, 268−273.

(29) Shi, Y.; Ervin, K. M. Catalytic Oxidation of Carbon Monoxide by Platinum Cluster Anions. *J. Chem. Phys.* **1998**, *108*, 1757−1760.

(30) Balaj, O. P.; Balteanu, I.; Rossteuscher, T. T. J.; Beyer, M. K.; Bondybey, V. E. Catalytic Oxidation of CO with N_2O on Gas-Phase Platinum Clusters. *Angew. Chem., Int. Ed.* **2004**, *43*, 6519−6522.
(31) Balteanu, I.; Balaj, O. P.; Beyer, M. K.; Bondybey, V. E. Reactions of Platinum Clusters $^{195}Pt_n^{\pm}$, n = 1−24, with N_2O Studied with Isotopically Enriched Platinum. *Phys. Chem. Chem. Phys.* **2004**, *6*, 2910−2913.
(32) Siu, C.-K.; Reitmeier, S. J.; Balteanu, I.; Bondybey, V. E.; Beyer, M. K. Catalyst Poisoning in the Conversion of CO and N_2O to CO_2 and N_2 on Pt_4^- in the Gas Phase. *Eur. Phys. J. D* **2007**, *43*, 189−192.
(33) Hermes, A. C.; Hamilton, S. M.; Cooper, G. A.; Kerpal, C.; Harding, D. J.; Meijer, G.; Fielicke, A.; Mackenzie, S. R. Infrared Driven CO Oxidation Reactions on Isolated Platinum Cluster Oxides, $Pt_nO_m^+$. *Faraday Discuss.* **2012**, *157*, 213−225.
(34) Rondinelli, F.; Russo, N.; Toscano, M. On the Pt^+ and Rh^+ Catalytic Activity in the Nitrous Oxide Reduction by Carbon Monoxide. *J. Chem. Theory Comput.* **2008**, *4*, 1886−1890.
(35) Lv, L.; Wang, Y.; Jin, Y. On the Catalytic Mechanism of $Pt_4^{\pm}$ in the Oxygen Transport Activation of N_2O by CO. *Theor. Chem. Acc.* **2011**, *130*, 15−25.
(36) Schlangen, M.; Schwarz, H. Effects of Ligands, Cluster Size, and Charge State in Gas-Phase Catalysis: A Happy Marriage of Experimental and Computational Studies. *Catal. Lett.* **2012**, *142*, 1265−1278.
(37) Kaldor, A.; Cox, D. M. Hydrogen Chemisorption on Gas-Phase Transition-Metal Clusters. *J. Chem. Soc., Faraday Trans.* **1990**, *86*, 2459−2463.
(38) Kummerlöwe, G.; Balteanu, I.; Sun, Z.; Balaj, O. P.; Bondybey, V. E.; Beyer, M. K. Activation of Methane and Methane-d_4 by Ionic Platinum Clusters. *Int. J. Mass Spectrom.* **2006**, *254*, 183−188.
(39) Trevor, D. J.; Whetten, R. L.; Cox, D. M.; Kaldor, A. Gas-Phase Platinum Cluster Reactions with Benzene and Several Hexanes: Evidence of Extensive Dehydrogenation and Size-Dependent Chemisorption. *J. Am. Chem. Soc.* **1985**, *107*, 518−519.
(40) Andersson, M.; Rosen, A. Catalytic Oxidation of Hydrogen on Free Platinum Clusters. *J. Chem. Phys.* **2002**, *117*, 7051−7054.
(41) Yamada, A.; Miyajima, K.; Mafuné, F. Catalytic Reactions on Neutral Rh Oxide Clusters More Efficient than on Neutral Rh Clusters. *Phys. Chem. Chem. Phys.* **2012**, *14*, 4188−4195.
(42) Sakuma, K.; Miyajima, K.; Mafuné, F. Oxidation of CO by Nickel Oxide Clusters Revealed by Post Heating. *J. Phys. Chem. A* **2013**, *117*, 3260−3265.
(43) Becke, A. D. Density-Functional Thermochemistry. III. The Role of Exact Exchange. *J. Chem. Phys.* **1993**, *98*, 5648−5652.
(44) Stephens, P. J.; Devlin, F. J.; Chablowski, C. F.; Frisch, M. J. Ab-Initio Calculation of Vibrational Absorption and Circular-Dichroism Spectra Using Density-Functional Force-Fields. *J. Phys. Chem.* **1994**, *98*, 11623−11627.
(45) Zhao, S.; Li, Z.; Wang, W.; Liu, Z.; Fan, K.; Xie, Y.; Schaefer, H. Is the Uniform Electron Gas Limit Important for Small Ag Clusters? Assessment of Different Density Functionals for Ag_n ($n \leq 4$). *J. Chem. Phys.* **2006**, *124*, 184102.
(46) Paier, J.; Marsman, M.; Kresse, G. Why Does the B3LYP Hybrid Functional Fail for Metals? *J. Chem. Phys.* **2007**, *127*, 024103.
(47) Weigend, F.; Ahlrichs, R. Balanced Basis Sets of Split Valence, Triple Zeta Valence and Quadruple Zeta Valence Quality for H to Rn: Design and Assessment of Accuracy. *Phys. Chem. Chem. Phys.* **2005**, *7*, 3297−3305.
(48) Frisch, M. J.; Trucks, G. W.; Schlegel, H. B.; Scuseria, G. E.; Robb, M. A.; Cheeseman, J. R.; Scalmani, G.; Barone, V.; Mennucci, B.; Petersson, G. A.; et al. *Gaussian 09*, revision A.02; Gaussian, Inc.: Wallingford, CT, 2009.
(49) Glendening, E. D.; Reed, A. E.; Carpenter, J. E.; Weinhold, F. *NBO Version 3.1*.
(50) Ohno, K.; Maeda, S. A Scaled Hypersphere Search Method for the Topography of Reaction Pathways on the Potential Energy Surface. *Chem. Phys. Lett.* **2004**, *384*, 277−282.
(51) Maeda, S.; Ohno, K. Global Mapping of Equilibrium and Transition Structures on Potential Energy Surfaces by the Scaled Hypersphere Search Method: Applications to ab Initio Surfaces of Formaldehyde and Propyne Molecules. *J. Phys. Chem. A* **2005**, *109*, 5742−5753.
(52) Ohno, K.; Maeda, S. Global Reaction Route Mapping on Potential Energy Surfaces of Formaldehyde, Formic Acid, and their Metal-Substituted Analogues. *J. Phys. Chem. A* **2006**, *110*, 8933−8941.
(53) Maeda, S.; Ohno, K. Structures of Water Octamers $(H_2O)_8$: Exploration on ab Initio Potential Energy Surfaces by the Scaled Hypersphere Search Method. *J. Phys. Chem. A* **2007**, *111*, 4527−4534.
(54) Kua, J.; Goddard, W. Chemisorption of Organics on Platinum. 1. the Interstitial Electron Model. *J. Phys. Chem. B* **1998**, *102*, 9481−9491.
(55) Li, T.; Balbuena, P. B. Computational Studies of the Interactions of Oxygen with Platinum Clusters. *J. Phys. Chem. B* **2001**, *105*, 9943−9952.
(56) Tian, W. Q.; Ge, M. F.; Sahu, B. R.; Wang, D. X.; Yamada, T.; Mashiko, S. Geometrical and Electronic Structure of the Pt_7 Cluster: A Density Functional Study. *J. Phys. Chem. A* **2004**, *108*, 3806−3812.
(57) Xiao, L.; Wang, L. C. Structures of Platinum Clusters: Planar or Spherical? *J. Phys. Chem. A* **2004**, *108*, 8605−8614.
(58) Bhattacharyya, K.; Majumder, C. Growth Pattern and Bonding Trends in Pt_n (n = 2−13) Clusters: Theoretical Investigation Based on First Principle Calculations. *Chem. Phys. Lett.* **2007**, *446*, 374−379.
(59) Fryburg, G.; Petrus, H. Kinetics of the Oxidation of Platinum. *J. Electrochem. Soc.* **1961**, *108*, 496−503.
(60) Krier, C.; Jaffee, R. Oxidation of the Platinum-Group Metals. *J. Less-Common Met.* **1963**, *5*, 411−431.
(61) Norman, J.; Staley, H.; Bell, W. Mass Spectrometric-Knudsen Cell Study of Gaseous Oxides of Platinum. *J. Phys. Chem.* **1967**, *71*, 3686−3689.
(62) Hannevold, L.; Nilsen, O.; Kjekshus, A.; Fjellvåg, H. Chemical Vapor Transport of Platinum and Rhodium with Oxygen as Transport Agent. *J. Cryst. Growth* **2005**, *279*, 206−212.
(63) Hannevold, L.; Nilsen, O.; Kjekshus, A.; Fjellvåg, H. Etching of Platinum-Rhodium Alloys in Oxygen-Containing Atmospheres. *J. Alloys Compd.* **2005**, *402*, 53−57.
(64) Herman, J.; Foutch, J. D.; Davico, G. E. Gas-Phase Reactivity of Selected Transition Metal Cations with CO and CO_2 and the Formation of Metal Dications Using a Sputter Ion Source. *J. Phys. Chem. A* **2007**, *111*, 2461−2468.
(65) Zakin, M. R.; Brickman, R. O.; Cox, D. M.; Kaldor, A. Dependence of Metal Cluster Reaction-Kinetics on Charge State I. Reaction of Neutral (Nb_x) and Ionic (Nb_x^+, Nb_x^-) Niobium Clusters with D_2. *J. Chem. Phys.* **1988**, *88*, 3555−3560.
(66) Cox, D.; Reichmann, K.; Trevor, D.; Kaldor, A. CO Chemisorption on Free Gas Phase Metal Clusters. *J. Chem. Phys.* **1988**, *88*, 111−119.